Phagocytosis model of calcium oxalate monohydrate crystals generated using human induced pluripotent stem cell-derived macrophages

Tomoki Okada
Nagoya City University Graduate School of Medical Sciences

Atsushi Okada
a-okada@med.nagoya-cu.ac.jp

Nagoya City University Graduate School of Medical Sciences

Hiromasa Aoki
Nagoya City University

Daichi Onozato
Nagoya City University

Taiki Kato
Nagoya City East Medical Center

Hiroshi Takase
Nagoya City University Graduate School of Medical Sciences

Shigeru Ohshima
Yokkaichi Nursing and Medical Technology school of Nursing and Medical Care

Teruaki Sugino
Nagoya City East Medical Center

Rei Unno
Nagoya City University Graduate School of Medical Sciences

Kazumi Taguchi
Nagoya City University Graduate School of Medical Sciences

Shuzo Hamamoto
Nagoya City University Graduate School of Medical Sciences

Ryosuke Ando
Nagoya City University Graduate School of Medical Sciences

Issei S Shimada
Nagoya City University Graduate School of Medical Sciences

Tadahiro Hashita
Nagoya City University

Takahiro Iwao

Nagoya City University

Tamihide Matsunaga

Nagoya City University

Takahiro Yasui

Nagoya City University Graduate School of Medical Sciences

Research Article

Additional Declarations: No competing interests reported.

Abstract

Macrophages play a role in nephrolithiasis, offering the possibility of macrophage-mediated preventive therapies. To establish a system for screening drugs that could prevent the formation of kidney stones, we aimed to develop a model using human induced pluripotent stem cell (iPSC)-derived macrophages to study phagocytosis of calcium oxalate monohydrate (COM) crystals. Human iPSCs (201B7) were cultured. CD14 + monocytes were recovered using a stepwise process that involved the utilization of growth factors and cytokines. These cells were then allowed to differentiate into M1 and M2 macrophages. The macrophages were co-cultured with COM crystals and used in the phagocytosis experiments. Live cell imaging using a super-resolution microscope was used to visualize phagocytosis. Intracellular fluorescence intensity was measured using imaging cytometry to quantify phagocytosis. Human iPSCs successfully differentiated into M1 and M2 macrophages. M1 macrophages adhered to the culture plate and moved COM crystals from the periphery to the center of the cell over time, whereas M2 macrophages did not adhere to the culture plate and actively phagocytosed the surrounding COM crystals. Fluorescence assessment over a 24-h period showed that M2 macrophages exhibited higher intracellular fluorescence intensity (5.65 times that of M1 macrophages at 4.5 h) and maintained this advantage for 18 h. This study revealed that human iPSC-derived macrophages have the capacity to phagocytose COM crystals, presenting a new approach for studying urinary stone formation and highlighting the potential of iPSC-derived macrophages as a valuable tool to screen drugs related to nephrolithiasis.

Introduction

The incidence of urinary stones is increasing on a global scale [1], and it has a major effect on global healthcare. The prevention of urinary stone formation is important, considering its negative effects on the health and quality of life of the affected individuals. Urinary stone formation is influenced by multiple factors, characterized by an interplay between genetic and environmental factors [2, 3]. The management of urinary mineral substances has been studied extensively to prevent stone formation; however, treatments that target genetic factors are lacking.

To investigate the genetic factors underlying urinary stone formation, we previously developed a mouse model that produces calcium oxalate monohydrate (COM) crystals in the kidney [4]. Stone elimination from the kidney was observed using microarray analysis, and it was attributed to phagocytosis of these crystals by macrophages [5, 6]. Macrophages include inflammatory type M1 and anti-inflammatory type M2 cells. M2-deficient mice demonstrate more renal crystal formation than wild-type mice, indicating that M2 macrophages could inhibit stone formation [7].

In humans, the numbers of crystals and macrophages in the renal papillae are higher in patients who have renal stones than in those who do not have renal stones [8]. A genome-wide analysis of Randall's plaques indicated upregulation of expression of monocyte-to-macrophage differentiation-associated genes in stone formers [9]. Considerable differences are observed in the levels of urinary interleukin (IL)-4,

IL-1a, granulocyte-macrophage colony-stimulating factor (GM-CSF), IL-1β, and IL-10 between patients with and without stone formation [10]. These findings strongly suggest that macrophages are related to urinary stone formation in humans. This discovery holds promise for the development of macrophage-mediated prevention of and dissolution therapies for urinary tract stones.

Drug discovery using macrophages requires screening of a large number of human macrophages, but the screening process is limited by the amount of peripheral blood that can be collected. In recent years, drug screening using induced pluripotent stem cells (iPSC) has yielded promising results in various disease fields [11, 12]. To delve deeper into this aspect, in this study, we aimed to establish a COM crystal phagocytosis model using iPSC-derived macrophages to develop a drug-screening system and observe the effect of differentiation of these cells into M1/M2 macrophages on COM phagocytosis.

Materials and Methods

iPSC cell culture

Human iPSCs (cell line 201B7) [13] were obtained from the Riken BioResource Research Center. iPSCs were maintained in mTeSR1 (ST-85850; STEMCELL Technologies, Ontario, Canada), a serum-free medium that does not require feeder cells, on tissue culture dishes coated with iMatrix-511 silk (892021; Takara Bio Inc., Shiga, Japan). The cells were maintained in a 5% CO_2 incubator set at 37°C and passaged with 0.5 mmol/L ethylenediaminetetraacetic acid every 4–5 days.

Differentiation of iPSCs into macrophages

The differentiation protocol for iPSC-derived monocytes was slightly modified from an earlier report (Fig. 1) [14]. The protocol consisted of four sequential steps. In Step 1, undifferentiated human iPSC colonies were cultured with 80 ng/mL bone morphogenetic protein 4 (314-BP; R&D Systems, Minneapolis, MN, USA) until they reached confluence. They were passaged and cultured for 4 days to induce the formation of primitive striated cells. In Step 2, the cells were cultured in StemPro-34 (10639011; Thermo Fisher Scientific, Waltham, MA, USA) supplemented with 2 mmol/L GlutaMAX (35050061; Thermo Fisher Scientific). The cells were treated with 80 ng/mL vascular endothelial growth factor (293-VE; R&D Systems), 25 ng/mL basic fibroblast growth factor (233-FB; R&D Systems), and 100 ng/mL stem cell factor (SCF) (255-SC; R&D Systems) for 3 days to induce differentiation into angioblast-like hematopoietic progenitor cells. In Step 3, the cells were treated with 50 ng/mL SCF, 50 ng/mL IL-3 (203-IL; R&D Systems), 5 ng/mL thrombopoietin (288-TP; R&D Systems), 50 ng/mL macrophage colony-stimulating factor (M-CSF) (216-MC; R&D Systems), and 50 ng/mL FMS-like tyrosine kinase 3 (Flt-3) (308-FK; R&D Systems) to induce differentiation into hematopoietic cells. The cells were cultured for 8 days, with a medium change on day 4. In Step 4, monocytes were cultured for 4 days with 50 ng/mL Flt-3, 50 ng/mL M-CSF, and 25 ng/mL GM-CSF (215-GM; R&D Systems). Positive sorting was performed using an autoMACS Pro Separator (Miltenyi Biotec, Bergisch Gladbach, Germany) with CD14 MicroBeads (130-050-201; Miltenyi Biotec) to extract CD14 + monocytes from the differentiated floating cells.

iPSCs were differentiated into primitive striated cells in Step 1; angioblast-like hematopoietic progenitors in Step 2; hematopoietic cells in Step 3; and monocytes in Step 4. Following the four steps, CD14 + monocytes were extracted and differentiated into non-polarized macrophages in Step 5 and into M1 and M2 macrophages in Step 6

The extracted CD14 + monocytes were allowed to differentiate into macrophages through the administration of M-CSF for 7 days, and then into M1 and M2 macrophages through 1-day administration of 20 ng/mL interferon-γ (285-IF; R&D Systems) and 20 ng/mL IL-4 (204-IL; R&D Systems), respectively (Fig. 1). For monocyte-to-macrophage differentiation, RPMI 1640 medium (11875093; Thermo Fisher Scientific) supplemented with 10% fetal bovine serum (FBS) (10437028; Thermo Fisher Scientific) was used.

Flow cytometric analysis

Flow cytometric analysis was performed using BD FACSCanto (BD Biosciences, Franklin Lakes, NJ, USA). CD14 was used as a marker of macrophages, HLA-DR as a marker of M1 macrophages, and CD206 as a marker of M2 macrophages. The differentiated macrophages were suspended at 2×10^6 cells in stain buffer (554656; BD Biosciences). Half of these cells were used as samples and the rest were used as isotype controls. Human BD Fc Block (564219; BD Biosciences) was added to each sample, and the samples were incubated at 4°C for 10 min. The samples were then treated with antibody (555399 APC Mouse Anti-Human CD14, 556643 FITC Mouse Anti-Human HLA-DR, 555954 PE Mouse Anti-Human CD206; BD Biosciences) and incubated at 4°C for 30 min. The samples were suspended in stain buffer for measurements and 7-AAD (559925; BD) was added immediately before measurement.

Preparation of normal and fluorescent COM crystals

COM crystals were prepared as described previously [15]. In brief, a mixture of sodium oxalate (200 mM, 0.5 mL) and calcium chloride (200 mM, 0.5 mL) was combined at room temperature (20°C) within a buffer solution comprising 90 mM Tris-HCl and 10 mM NaCl, adjusted to pH 7.4. The final concentration of the mixture was adjusted to 10 mM. The COM crystals were allowed to equilibrate for 3 days and then washed three times with phosphate-buffered saline (PBS). The crystals were saturated with calcium oxalate and resuspended to attain a final concentration of 2.92 mg/mL. The pH was adjusted to 6.8.

Fluorescent labeling of the prepared COM crystals (f-COM) was performed according to the method of Chaiyarit et al. [16]. A mixture of 5 mmol/L $CaCl_2$ and 0.5 mmol/L sodium oxalate was prepared in a buffer solution comprising 90 mmol/L Tris-HCl, 10 mmol/L NaCl, and 0.11 µg/mL AlexaFluor 488 goat anti-mouse IgG (ab150113; Abcam, Cambridge, UK) at a pH of 7.4. The COM crystals were collected through centrifugation at 2000 × g for 5 min. The supernatant was removed, and the COM crystals were resuspended in methanol and centrifuged at 2000 × g for 5 min. Methanol was discarded, and the crystals were allowed to air-dry overnight at room temperature (20°C).

Live imaging of phagocytosis of COM crystals by iPSC-derived macrophages using super-resolution microscopy

iPSC-derived M1 and M2 macrophages were cultured in RPMI 1640 medium supplemented with 10% FBS and 1% penicillin–streptomycin (PS) (15140122; Thermo Fisher Scientific). The macrophages were added to six-well plates as a cell suspension at 1×10^5 cells/mL. COM crystals (375 µg) were added to each well. Thereafter, live cell imaging was performed using the SpinSR10 Super-resolution microscope (Evident, Tokyo, Japan), and continuous image capturing was performed every 15 min for 6 h under ambient room conditions at 37°C.

Quantifying phagocytosis of f-COM crystals by iPSC-derived macrophages using imaging cytometry

CellTracker (C34551; Thermo Fisher Scientific) and Hoechst 33342 (H1399; Thermo Fisher Scientific) were added to PBS (10 µM staining solution). iPSC-derived macrophages were collected and incubated in the staining solution for 45 min under 5% CO2 at 37°C. The cells were stored in RPMI 1640 supplemented with 10% FBS and 1% PS. M1 and M2 macrophages were prepared as cell suspensions at a density of 1×10^5 cells/mL and seeded in six-well plates. The prepared f-COM crystals (375 µg) were then added to each well. Wells with only macrophages and wells with only f-COM were used as controls. Live cell imaging was performed using In Cell Analyzer 6000 (Molecular Devices, San Jose, CA, USA) to quantify the fluorescence from Alexa Fluor 488 (ab150113; Abcam) conjugated to the f-COM crystals within the macrophages. Quantification was performed by scanning 15 fields-of-view for evaluating the fluorescence of f-COM crystals in each of the 6 wells. This scanning was performed continuously every 30 min for 24 h (1,440 min). After scanning all images, the total fluorescence intensity of f-COM incorporated into the macrophages was measured and divided by the number of cells to quantify the amount of phagocytosis per cell. This value was defined as the intracellular fluorescence intensity and was calculated every 30 min.

Results

Confirmation of differentiation into iPSC-derived macrophages using flow cytometry

M1 and M2 macrophages were derived from iPSCs using the protocol shown in Fig. 1. After the four steps, CD14 + monocytes extracted using autoMACS were sorted using flow cytometry. The extracted CD14 + monocytes successfully differentiated into M1 and M2 macrophages. Flow cytometry was used to assess the expression of representative macrophage surface markers, such as CD14, HLA-DR, and CD206. Expression of these markers exhibited distinctive outcomes in M1 and M2 macrophages (Fig. 2).

Live imaging of COM crystal phagocytosis by iPSC-derived macrophages using super-resolution microscopy

M1 and M2 macrophages derived from iPSCs phagocytosed the surrounding COM crystals. However, the mode of phagocytosis differed between M1 and M2 macrophages. M1 macrophages adhered to the plate

without migrating, and the phagocytosed crystals moved intracellularly from the periphery toward the center of the cells over time (Fig. 3A). In contrast, M2 macrophages did not adhere to the plate and phagocytosed the surrounding COM crystals during migration (Fig. 3B). Sequential movies are provided in supplementary Fig. 1A, B.

Quantifying phagocytosis of f-COM crystals by iPSC-derived macrophages using imaging cytometry

Fluorescently labeled iPSC-derived M1 and M2 macrophages phagocytosed f-COM crystals and incorporated them inside (Fig. 4A, B). The maximum total cell count in the 15 scanned fields-of-view was 10^7 cells for M1 macrophages and 97 cells for M2 macrophages. The 24-h measurement showed a gradual decrease in the cell count (up to 51 cells for M1 macrophages and 37 cells for M2 macrophages; Fig. 5A). The intracellular fluorescence intensity of M2 macrophages reached the maximum at 4.5 h from the start of the measurements, approximately 5.65 times higher than that observed for M1 macrophages for the same period. M2 macrophages showed higher intracellular fluorescence intensity than M1 macrophages, up to 18 h from the start of the measurements; however, thereafter, the intensity was similar (Fig. 5B).

Discussion

Phagocytosis of COM crystals by iPSC-derived macrophages was investigated in this study. Flow cytometry was used to confirm the differentiation of iPSCs into M1 and M2 macrophages. Live cell imaging was used to visualize the phagocytosis of COM crystals by macrophages and quantify the phagocytic activity. This approach revealed that M2 macrophages demonstrated higher phagocytosis of COM crystals than M1 macrophages.

Previous in vitro studies have confirmed crystal phagocytosis over time using mouse J774.1 macrophages [17]. Human macrophages differentiated using M-CSF showed a greater ability to phagocytose crystal deposits than those treated with GM-CSF [18]. Therefore, macrophages play an important role in nephrolithiasis by removing and digesting interstitial renal crystal deposits. Randall's plaques observed on the surface of the renal papillae are the sites of renal stone formation [19]. A genome-wide gene expression analysis of Randall's plaques suggested an association between macrophage activation and inflammatory cytokines [9]. In addition, Randall's plaques are associated with the presence of large, classically activated M1 macrophages and downregulation of alternatively activated M2 macrophages in the surrounding renal tissues [20]. Signaling mechanisms that promote the polarization of macrophages toward M2 phenotypes include the NLRP3, PPARγ-miR-23-Irf1/Pknox1, miR-93-TLR4/IRF1, and miR-185-5p/CSF1 pathways [21]. These results suggest therapeutic strategies for preventing stone formation by specifically promoting M2 macrophage development and enhancing crystal phagocytosis.

No previous study has used iPSC-derived macrophages to establish a model for COM crystal phagocytosis or demonstrated that iPSC-derived macrophages have a phagocytic capacity for COM crystals. The findings of the present study suggest the potential of using iPSC technology to develop a screening system for drugs aimed at preventing urinary stones. iPSC-based drug screening has already been performed for neurological disorders (including Alzheimer's disease), liver disease, and spinal cord injury [22].

Considering the origin of macrophages in research is important. For instance, the genetic background differs between mouse and human macrophages [23]. Monocytes can be isolated from human peripheral blood and can be differentiated into macrophage [24]; however, the amount of macrophages produced using this method is limited. Several reports on the generation of iPSC-derived macrophages have been published [25, 26]; using this method, a large number of macrophages can be generated for an extended period [12]. In terms of the availability of sufficient numbers of macrophages, iPSC-derived macrophages are a valuable tool for studying macrophage-mediated therapies in urinary stone formation.

This study has several limitations. First, iPSC-derived macrophages were used as an in vitro model. iPSCs can form a variety of cells, including macrophages; however, their behavior and characteristics may not fully reflect the complex in vivo environment. Therefore, the results of the present study must be further validated in vivo and in humans. In addition, organoids that mimic renal tissue, derived from iPSCs, can be used for validation. Second, we employed COM crystals for phagocytosis evaluation. COM is the most common component of urinary stones; however, the composition and growth process of stones in vivo in patients are complex. Future studies should examine other components of the stones to understand macrophage behavior during stone formation more comprehensively. Third, the iPSCs used in this study were derived from healthy individuals. There may be differences in the phagocytosis of urinary stones by macrophages generated from patient-derived iPSCs. Therefore, disease-specific iPSCs should be examined in future studies.

Conclusions

This study revealed that iPSC-derived macrophages have a phagocytic capacity for COM crystals. Therefore, this study presented a new approach for studying urinary stone formation and highlighted the potential of iPSC-derived macrophages as a valuable tool for screening drugs aimed at preventing urinary stone formation.

Declarations

Compliance with Ethical Standards

Disclosure of potential conflicts of interest

The authors declare that they have no conflict of interest.

Research involving Human Participants and/or Animals

Not applicable.

Informed consent

Consent to participate

Not applicable.

Consent to publish

Not applicable.

Data Availability

The datasets generated and analyzed during the current study are available from the corresponding author on reasonable request.

Code Availability

Not applicable.

References

1. Lang J, Narendrula A, El-Zawahry A, Sindhwani P, Ekwenna O (2022) Global trends in incidence and burden of urolithiasis from 1990 to 2019: an analysis of global burden of disease study data. Eur Urol Open Sci 35:37–46. https://doi.org/10.1016/j.euros.2021.10.008

2. Howles SA, Thakker RV (2020) Genetics of kidney stone disease. Nat Rev Urol 17:407–421. https://doi.org/10.1038/s41585-020-0332-x. Epub 2020 Jun 12

3. Zisman AL (2017) Effectiveness of treatment modalities on kidney stone recurrence. Clin J Am Soc Nephrol 12:1699–1708. https://doi.org/10.2215/CJN.11201016. Epub 2017 Aug 22

4. Okada A, Nomura S, Higashibata Y, Hirose M, Gao B, Yoshimura M, et al (2007) Successful formation of calcium oxalate crystal deposition in mouse kidney by intraabdominal glyoxylate injection. Urol Res 35:89–99. https://doi.org/10.1007/s00240-007-0082-8. Epub 2007 Febr 14

5. Okada A, Yasui T, Hamamoto S, Hirose M, Kubota Y, Itoh Y, et al (2009) Genome-wide analysis of genes related to kidney stone formation and elimination in the calcium oxalate nephrolithiasis model mouse: detection of stone-preventive factors and involvement of macrophage activity. J Bone Miner Res 24:908–924. https://doi.org/10.1359/jbmr.081245

6. Okada A, Yasui T, Fujii Y, Niimi K, Hamamoto S, Hirose M, et al (2011) Renal macrophage migration and crystal phagocytosis via inflammatory-related gene expression during kidney stone formation and elimination in mice: detection by association analysis of stone-related gene expression and microstructural observation. J Bone Miner Res:2701–2711. https://doi.org/10.1002/jbmr.158. Epub 2010 Jun 23. Erratum in: J Bone Miner Res (2011) 26:439. https://doi.org/10.1002/jbmr.334

7. Taguchi K, Okada A, Kitamura H, Yasui T, Naiki T, Hamamoto S, et al (2014) Colony-stimulating factor-1 signaling suppresses renal crystal formation. J Am Soc Nephrol 25:1680–1697. https://doi.org/10.1681/ASN.2013060675. Epub 2014 Febr 27

8. Okada A, Hamamoto S, Taguchi K, Unno R, Sugino T, Ando R, et al (2018) Kidney stone formers have more renal parenchymal crystals than non-stone formers, particularly in the papilla region. BMC Urol 18:19. https://doi.org/10.1186/s12894-018-0331-x

9. Taguchi K, Hamamoto S, Okada A, Unno R, Kamisawa H, Naiki T, et al (2017) Genome-wide gene expression profiling of Randall's plaques in calcium oxalate stone formers. J Am Soc Nephrol 28:333–347. https://doi.org/10.1681/ASN.2015111271. Epub 2016 Jun 13

10. Okada A, Ando R, Taguchi K, Hamamoto S, Unno R, Sugino T, et al (2019) Identification of new urinary risk markers for urinary stones using a logistic model and multinomial logit model. Clin Exp Nephrol 23:710–716. https://doi.org/10.1007/s10157-019-01693-x. Epub 2019 Jan 18

11. Elitt MS, Barbar L, Tesar PJ (2018) Drug screening for human genetic diseases using iPSC models. Hum Mol Genet 27:R89–98. https://doi.org/10.1093/hmg/ddy186

12. Gutbier S, Wanke F, Dahm N, Rümmelin A, Zimmermann S, Christensen K, et al (2020) Large-scale production of human iPSC-derived macrophages for drug screening. Int J Mol Sci 21:4808. https://doi.org/10.3390/ijms21134808

13. Takahashi K, Tanabe K, Ohnuki M, Narita M, Ichisaka T, Tomoda K, Yamanaka S (2007) Induction of pluripotent stem cells from adult human fibroblasts by defined factors. Cell 131:861–872. https://doi.org/10.1016/j.cell.2007.11.019

14. Yanagimachi MD, Niwa A, Tanaka T, Honda-Ozaki F, Nishimoto S, Murata Y, et al (2013) Robust and highly-efficient differentiation of functional monocytic cells from human pluripotent stem cells under

serum- and feeder cell-free conditions. PLOS ONE 8:e59243. https://doi.org/10.1371/journal.pone.0059243. Epub 2013 Apr 3

15. Zuo L, Tozawa K, Okada A, Yasui T, Taguchi K, Ito Y, et al (2014) A paracrine mechanism involving renal tubular cells, adipocytes and macrophages promotes kidney stone formation in a simulated metabolic syndrome environment. J Urol 191:1906–1912. https://doi.org/10.1016/j.juro.2014.01.013. Epub 2014 Febr 8

16. Chaiyarit S, Mungdee S, Thongboonkerd V (2010) Nonradioactive labelling of calcium oxalate crystals for investigations of crystal-cell interaction and internalization. Anal Methods 2:1536–1541. https://doi.org/10.1039/C0AY00321B

17. Okada A, Aoki H, Onozato D, Kato T, Hashita T, Takase H, et al (2019) Active phagocytosis and diachronic processing of calcium oxalate monohydrate crystals in an in vitro macrophage model. Kidney Blood Press Res 44:1014–1025. https://doi.org/10.1159/000501965. Epub 2019 Sep 11

18. Kusmartsev S, Dominguez-Gutierrez PR, Canales BK, Bird VG, Vieweg J, Khan SR (2016) Calcium oxalate stone fragment and crystal phagocytosis by human macrophages. J Urol 195:1143–1151. https://doi.org/10.1016/j.juro.2015.11.048. Epub 2015 Nov 26

19. Evan A, Lingeman J, Coe FL, Worcester E (2006) Randall's plaque: pathogenesis and role in calcium oxalate nephrolithiasis. Kidney Int 69:1313–1318. https://doi.org/10.1038/sj.ki.5000238

20. Khan SR, Canales BK, Dominguez-Gutierrez PR (2021) Randall's plaque and calcium oxalate stone formation: role for immunity and inflammation. Nat Rev Nephrol 17:417–433. https://doi.org/10.1038/s41581-020-00392-1. Epub 2021 Jan 29

21. Taguchi K, Okada A, Unno R, Hamamoto S, Yasui T (2021) Macrophage function in calcium oxalate kidney stone formation: A systematic review of literature. Front Immunol 12:673690. https://doi.org/10.3389/fimmu.2021.673690

22. Aboul-Soud MAM, Alzahrani AJ, Mahmoud A (2021) Induced pluripotent stem cells (iPSCs)-roles in regenerative therapies, disease modelling and drug screening. Cells 10:2319. https://doi.org/10.3390/cells10092319

23. Ingersoll MA, Spanbroek R, Lottaz C, Gautier EL, Frankenberger M, Hoffmann R, et al (2010) Comparison of gene expression profiles between human and mouse monocyte subsets. Blood;115(3):e10–19. https://doi.org/10.1182/blood-2009-07-235028. Epub 2009 Nov 12. Erratum in: Blood (2010) 116:857. https://doi.org/10.1182/blood-2010-06-290122

24. Nielsen MC, Andersen MN, Møller HJ (2020) Monocyte isolation techniques significantly impact the phenotype of both isolated monocytes and derived macrophages in vitro. Immunology 159:63–74. https://doi.org/10.1111/imm.13125. Epub 2019 Nov 27

25. Mukherjee C, Hale C, Mukhopadhyay S (2018) A simple multistep protocol for differentiating human induced pluripotent stem cells into functional macrophages. Methods Mol Biol 1784:13–28. https://doi.org/10.1007/978-1-4939-7837-3_2

26. Shi J, Xue C, Liu W, Zhang H (2019) Differentiation of human-induced pluripotent stem cells to macrophages for disease modeling and functional genomics. Curr Protoc Stem Cell Biol 48:e74.
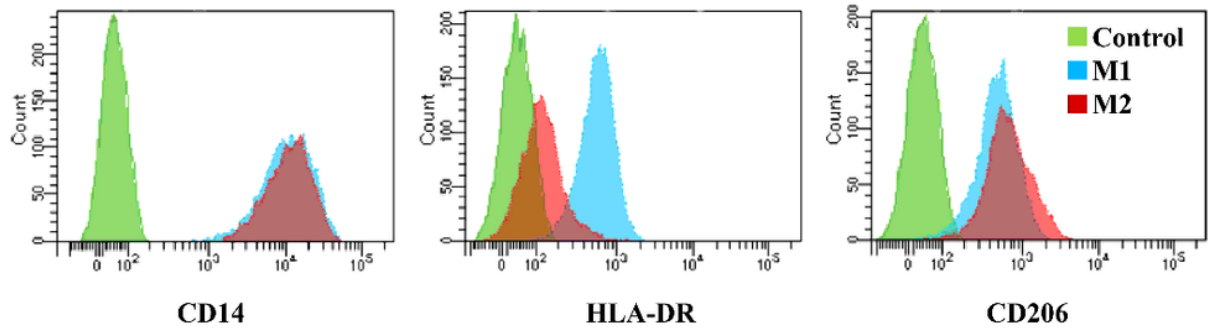
Figures
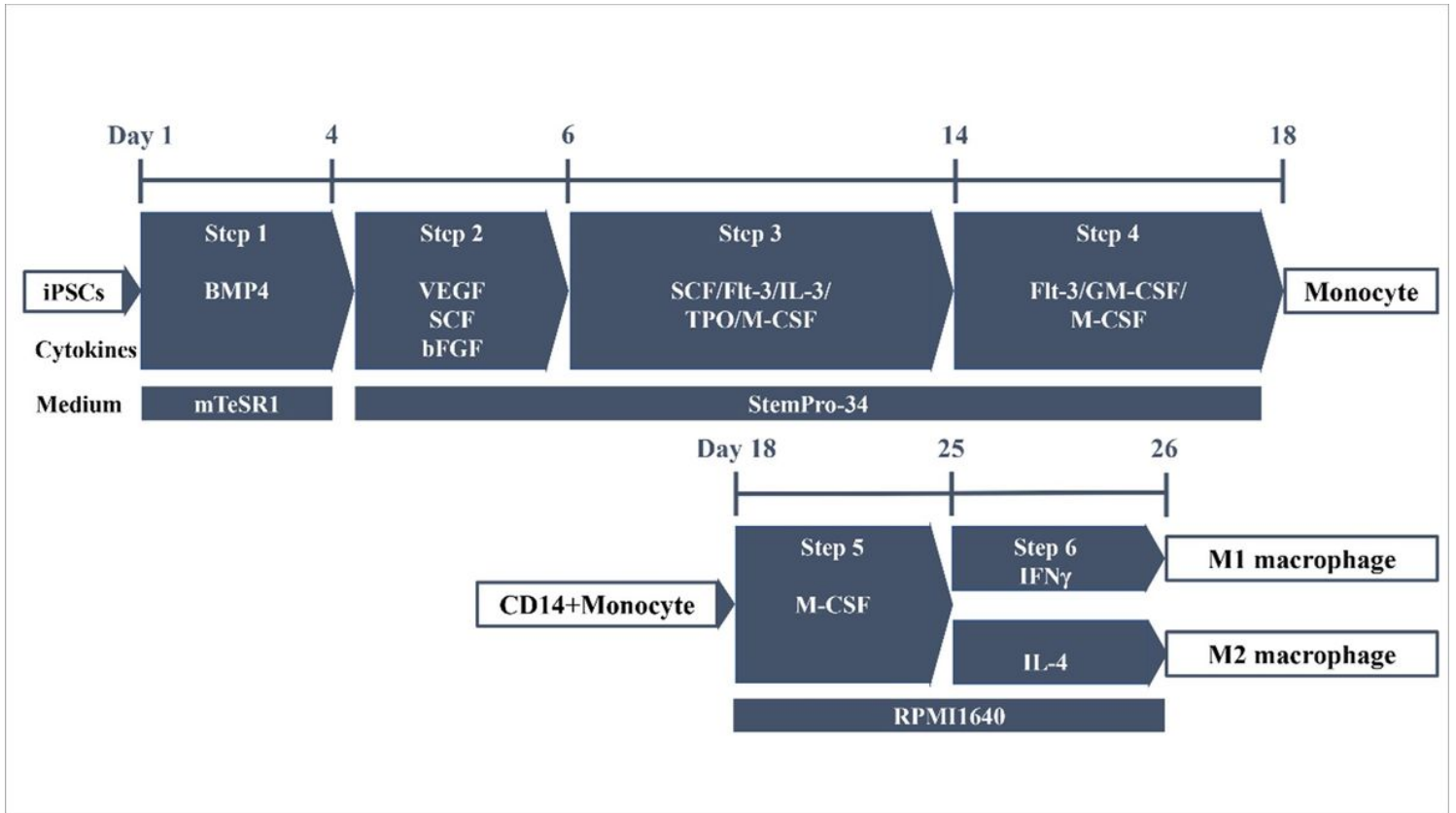
Figure 1

Differentiation scheme showing the different steps, including the administration of cytokines and growth factors, and the medium conditions used to obtain monocytes and macrophages from induced pluripotent stem cells (iPSCs)

iPSCs were differentiated into primitive striated cells in Step 1; angioblast-like hematopoietic progenitors in Step 2; hematopoietic cells in Step 3; and monocytes in Step 4. Following the four steps, CD14+ monocytes were extracted and differentiated into non-polarized macrophages in Step 5 and into M1 and M2 macrophages in Step 6

Figure 2

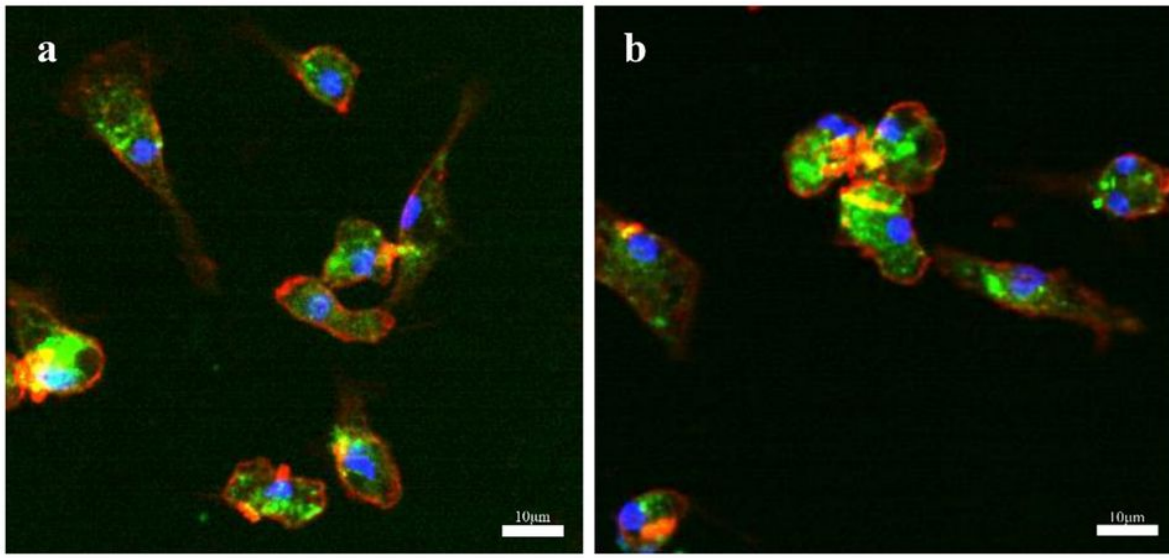Flow cytometry of induced pluripotent stem cell-derived macrophages

Expression of cell surface markers indicated in green for negative controls with isotype control, blue for M1 macrophages, and red for M2 macrophages
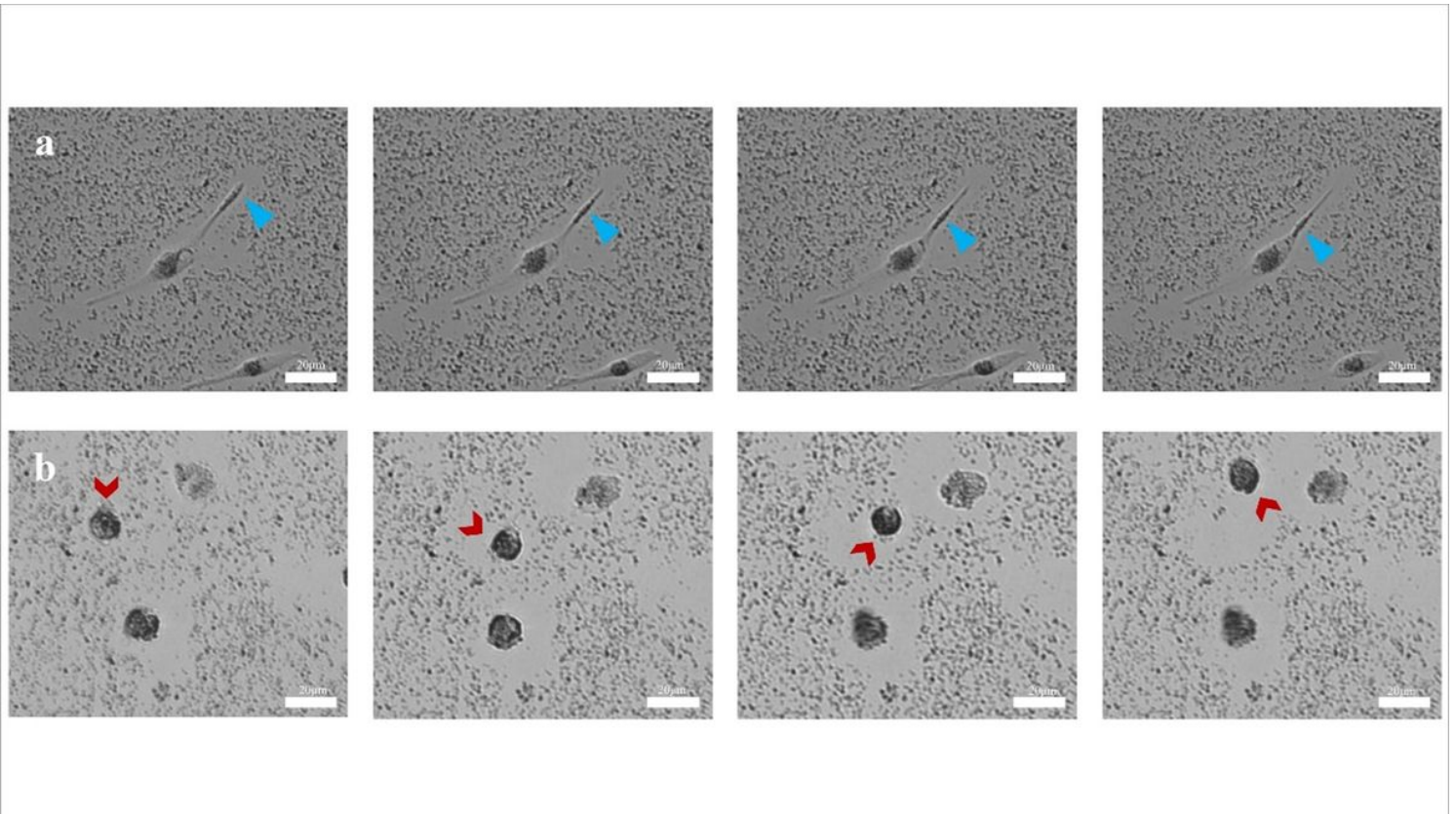
Figure 3

Live cell imaging data captured during the phagocytosis of calcium oxalate monohydrate (COM) crystals by induced pluripotent stem cell-derived macrophages
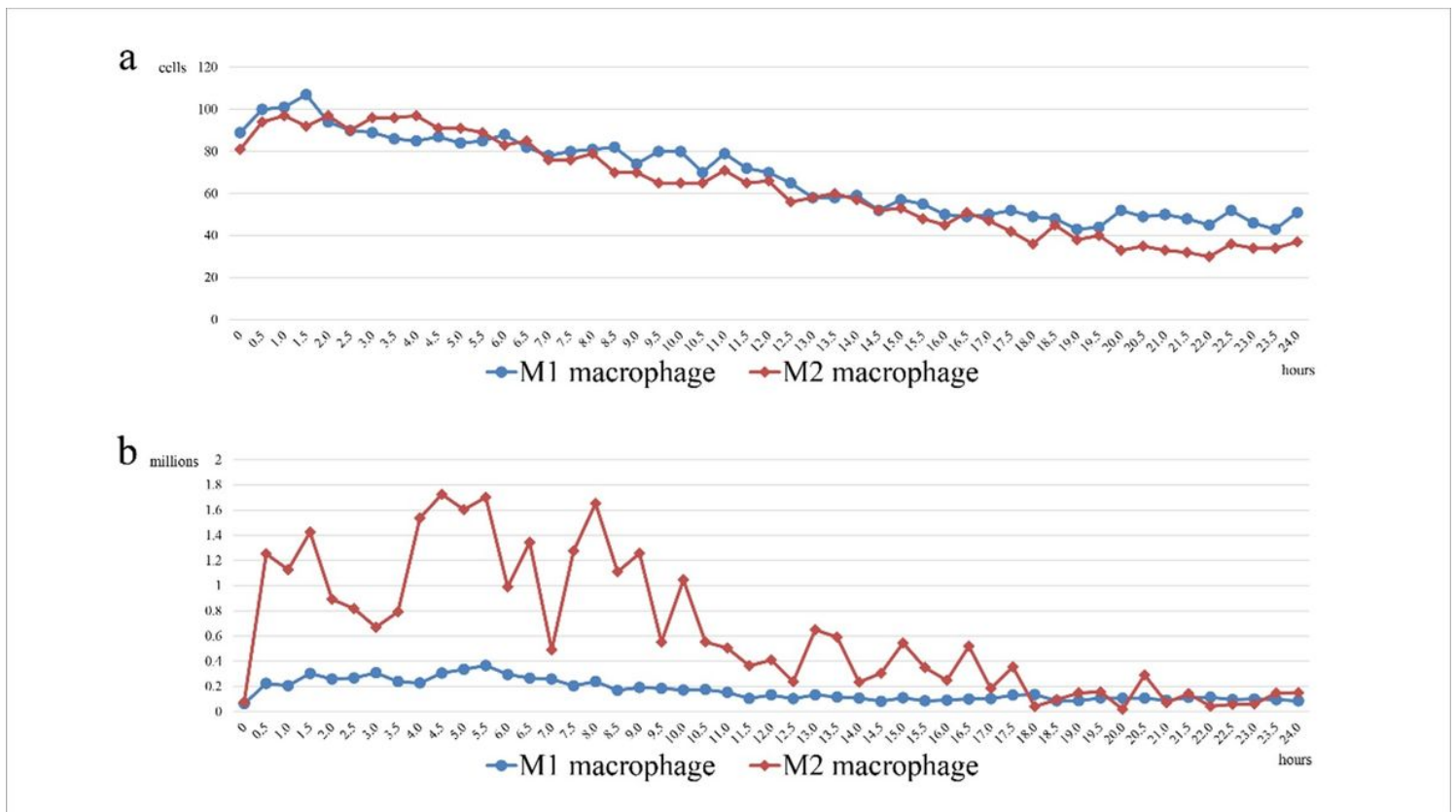
(a) COM crystals phagocytosed by M1 macrophages (indicated by blue arrowhead) migrating from the periphery toward the center were imaged every 120 min (360 min in total). (b) M2 macrophages actively migrating in the direction of the red arrowhead; phagocytosed and disappearing COM crystals were imaged every 120 min (360 min in total)

Figure 4

Phagocytosis of fluorescent COM crystals by induced pluripotent stem cell-derived macrophages

(a) M1 macrophages and (b) M2 macrophages. Green fluorescence indicates fluorescent COM (f-COM) crystals. Red fluorescence indicates cell membrane. Blue fluorescence indicates nucleus

Figure 5

Quantification of phagocytosis of fluorescent COM crystals by induced pluripotent stem cell-derived macrophages

Blue graph shows M1 macrophages and red graph shows M2 macrophages. (a) Decreased number of M1 and M2 macrophages measured over 24 h of co-culture with f-COM crystals. (b) Total fluorescence of phagocytosed f-COM crystals divided by the number of cells was used to determine the amount of phagocytosis per cell. This value was recorded every 30 min for 24 h and was defined as the intracellular fluorescence intensity

Supplementary Files

This is a list of supplementary files associated with this preprint. Click to download.

- SupplementalData1a.mp4
- SupplementalData1b.mp4